10-2017

Racemic and Enantiopure Forms of 3-Ethyl-3-Phenylpyrrolidin-2-One Adopt Very Different Crystal Structures

Arcadius V. Krivoshein
University of Houston, Clear Lake

Sergey V. Lindeman
Marquette University, sergey.lindeman@marquette.edu

Tatiana V. Timofeeva
New Mexico Highlands University

Victor N. Khrustalev
Russian Academy of Sciences

Chirality, Vol. 29, No. 10 (October 2017): 623-633. DOI.

Racemic And Enantiopure Forms Of 3-Ethyl-3-Phenylpyrrolidin-2-One Adopt Very Different Crystal Structures

Arcadius V. Krivoshein
Department of Physical & Applied Sciences, University of Houston – Clear Lake, Houston, Texas
Sergey V. Lindeman
Department of Chemistry, Marquette University, Milwaukee, Wisconsin
Tatiana V. Timofeeva
Department of Chemistry, New Mexico Highlands University, Las Vegas, New Mexico
Victor N. Khrustalev
Department of Chemistry, New Mexico Highlands University, Las Vegas, New Mexico
Department of Inorganic Chemistry, Peoples' Friendship University of Russia, Moscow, Russia

Abstract

3-Ethyl-3-phenylpyrrolidin-2-one *(*EPP) is an experimental anticonvulsant based on the newly proposed α-substituted amide group pharmacophore. These compounds show robust activity in animal models of drug-resistant epilepsy and are thus promising for clinical development. In order to understand pharmaceutically

relevant properties of such compounds, we are conducting an extensive investigation of their structures in the solid state. In this article, we report chiral high-performance liquid chromatography (HPLC) separation, determination of absolute configuration of enantiomers, and crystal structures of EPP. Preparative resolution of EPP enantiomers by chiral HPLC was accomplished on the Chiralcel OJ stationary phase in the polar-organic mode. Using a combination of electronic CD spectroscopy and anomalous dispersion of X-rays we established that the first-eluted enantiomer corresponds to (+)-(*R*)-EPP, while the second-eluted enantiomer corresponds to (−)-(*S*)-EPP. We also demonstrated that, in the crystalline state, enantiopure and racemic forms of this anticonvulsant have considerable differences in their supramolecular organization and patterns of hydrogen bonding. These stereospecific structural differences can be related to the differences in melting points and, correspondingly, solubility and bioavailability.

1 INTRODUCTION

Chiral factors have long been known to play an important role in biological activity.[1] However, the interplay between chiral factors and drug polymorphism in the solid state is less explored. Nevertheless, it is clear that the differing crystal structures (and, therefore, differing physicochemical properties) of polymorphic modifications of racemates and enantiomers can have profound implications on pharmaceutical manufacturing, stability upon storage, and pharmacokinetics of solid dosage forms.[2]

Epileptic seizures result from the imbalance between excitation and inhibition in the brain. Epilepsy is the most widespread type of neurological disorder—it affects about 70 million people worldwide.[3] Despite many available antiepileptic drugs (AEDs), drug resistance and side effects remain the two main challenges in the pharmacotherapy of epilepsy. Therefore, the search for new AEDs and improved pharmaceutical formulations of existing AEDs continues. In the course of our studies of drugs affecting neurotransmitter receptors in the brain, our attention has recently turned to α-substituted acetamides, lactams, and cyclic imides.[4]

Racemic 3-ethyl-3-phenylpyrrolidin-2-one (EPP; Figure **1**) is the most active of the several α-substituted pyrrolidin-2-ones synthesized by Marshall in the late 1950s.[5] Subsequently, it was tested in epileptic patients with promising results.[6] Our own recent studies indicate that in animal tests this compound is active not only in conventional but also in drug-resistant models of epilepsy (to be published elsewhere), suggesting that it is a promising lead for further drug development. Since EPP is a chiral molecule, its *R* and *S* enantiomers in solution may differ in pharmacological activity, and its racemic and enantiopure forms in the solid state may differ in solubility and bioavailability. Therefore, as part of our comprehensive studies of the solid-state properties of α-substituted acetamides, lactams, and cyclic imides, it was of interest to determine the absolute configuration of EPP enantiomers and to examine the solid-state structure of enantiopure and racemic forms of this compound.

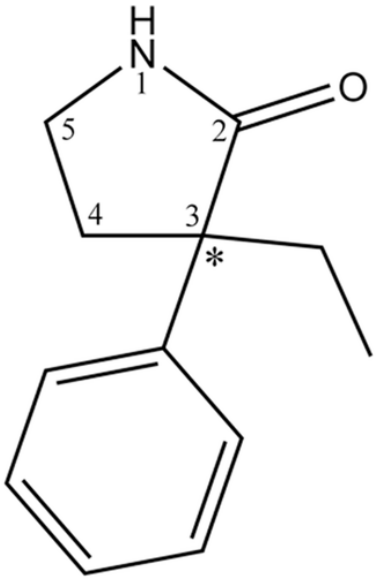

Figure 1 Structure of 3-ethyl-3-phenylpyrrolidin-2-one (EPP). The chiral carbon atom is indicated by an asterisk

2 MATERIALS AND METHODS

2.1 General

Rac-EPP (TCS 9875–02, lot BK-14-CR5296) was custom synthesized for us by Tocris Cookson (Bristol, UK). Methanol and acetonitrile (OmniSolv, HPLC gradient grade), acetone (ACS grade), and hexanes (ACS grade) were from EMD Millipore (Billerica, MA).

Melting curves were recorded in the OptiMelt MPA100 automated melting point system controlled by MeltView v. 1.107 software (Stanford Research Systems, Sunnyvale, CA) with a heating rate of 1 °C/min.

2.2 Chiral HPLC

Preparative high-performance liquid chromatography (HPLC) resolution of EPP enantiomers in the polar-organic mode was accomplished at room temperature (20–22 °C) on a Chiralcel OJ-H (10 × 250 mm) column (Daicel, Osaka, Japan) using neat MeOH as an eluent at flow rate of 1 ml/min. A Breeze 2 HPLC system (Waters, Milford, MA), consisting of a model 1525 binary pump and model 2707 autosampler with 500-µl sample loop and connected to an Altex model 152 UV detector (Beckman Coulter, Indianapolis, IN) fitted with a preparative (0.5-mm pathlength) flow cell and set at 254 nm, was used. The collected fractions were dried *in vacuo* and recrystallized from 15 mg/ml solutions in hexanes/acetone (2:1) at room temperature (20–22 °C) in a desiccator in order to produce samples used in all experiments described in this article.

Enantiomeric purity of the resolved enantiomers was confirmed by analytical chiral HPLC at room temperature (20–22 °C) on a Chiralcel OJ-H (4.6 × 250 mm) column (Daicel) operated in the reversed-phase mode. The elution was accomplished using a gradient of AcCN in H_2O (from 14.5% to 90.5% of AcCN in 16 min at a flow rate of 0.3 ml/min). A 1260 Infinity UHPLC system (Agilent Technologies, Santa Clara, CA) consisting of a 1260 µ-degasser, 1260 binary pump, 1260 ALS standard autosampler with 100-µl analytical head, 1260 TCC thermostatted column compartment, and 1260 DAD VL+ photodiode array UV–Vis detector set at 258 nm, was used.

2.3 Circular dichroism (CD) spectroscopy

Far-UV CD spectra of 1-mM solutions of EPP enantiomers in AcCN/H_2O (1:1) were recorded at room temperature (20–22 °C) in a 1-mm pathlength quartz optical cell on a J-815 CD spectrometer (Jasco, Easton,

MD). The instrumental settings were as follows: 5-nm spectral bandwidth, 100 nm/min scan speed, and 1-s data integration time (DIT).

2.4 IR spectroscopy

Infrared spectra of finely ground crystals were recorded at room temperature (20–22 °C) on a Nicolet iS10 FT-IR spectrometer fitted with a Smart iTR single-reflection ZnSe ATR accessory (Thermo Scientific, Waltham, MA). The instrumental settings were as follows: spectral range 4000–650 cm^{-1}, resolution 2 cm^{-1}, 32 spectra collected and averaged for each sample, and 64 spectra—for each background (with the automatic atmospheric suppression enabled). Omnic v. 8.3.103 software (Thermo Scientific) was used to record the spectra and apply Advanced ATR Correction and linear baseline correction.

2.5 Single-crystal x-ray diffraction analysis

The data for *rac*-EPP were collected at 100 K on a Bruker-AXS SMART APEX II CCD diffractometer using graphite-monochromatized MoKα radiation (λ = 0.71073 Å) and corrected for absorption using the SADABS program. The data for (+)-(*R*)-EPP and (+)-(*S*)-EPP were collected at 100 K on an Oxford SuperNova Atlas CCD diffractometer using graphite-monochromatized CuKα radiation (λ = 1.54184 Å) and corrected for absorption using the CrysAlisPRO program.

The crystal structures were solved by direct methods and refined by a full-matrix least-squares technique on F^2 with anisotropic displacement parameters for nonhydrogen atoms. The hydrogen atoms at nitrogens were objectively localized in the difference Fourier maps and refined with fixed isotropic displacement parameters: $U_{iso}(H) = 1.2U_{eq}(N)$. The hydrogen atoms at carbons were placed in calculated positions and included in the refinement within the riding model with fixed isotropic displacement parameters: $U_{iso}(H) = 1.5U_{eq}(C)$ for CH_3 groups and $1.2U_{eq}(C)$ for other groups. All calculations were carried out using the SHELX program[7] running under Olex2 GUI[8] (OlexSys, Durham, UK).

The absolute configuration of the chromatographically resolved enantiomers was determined based on anomalous dispersion intensities described by the Flack *x* parameter[9] or Hooft *y* parameter.[10] The Flack parameter was calculated in SHELX during the refinement, while the Hooft parameter was calculated postrefinement in PLATON.[11]

The atomic coordinates have been deposited with the Cambridge Crystallographic Data Center: CCDC 1530630 entry for (+)-(*R*)-EPP, CCDC 1530631 for (−)-(*S*)-EPP, and CCDC 1530629 entry for *rac*-EPP. These data can be obtained free of charge from the Director, CCDC, 12 Union Road, Cambridge CB2 1EZ, UK (e-mail: deposit@ccdc.cam.ac.uk; website: www.ccdc.cam.ac.uk).

3 RESULTS AND DISCUSSION

3.1 Resolution of EPP enantiomers by chiral HPLC

Chiral resolution (chromatographically or by other means) of EPP has not been reported so far. In our previous work,[12] we successfully used chiral HPLC in the reversed-phase mode to separate enantiomers of 2-phenylbutyramide and 3-methyl-3-phenylpyrrolidine-2,5-dione on a gram scale. However, the relatively low aqueous solubility of EPP made it impractical to use the reversed-phase mode in this study. We therefore attempted to separate the EPP enantiomer in the polar-organic mode.[13, 14] Preliminary experiments with Chiralcel OD or Chiralcel OJ as stationary phases and AcCN or MeOH as mobile phases (not shown) indicated that the best separation is achieved using the Chiralcel OJ stationary phase with MeOH as the mobile phase. The separation was scaled up to separate 10 mg of racemic EPP in each run on a 10 × 250 mm column (Figure **2**).

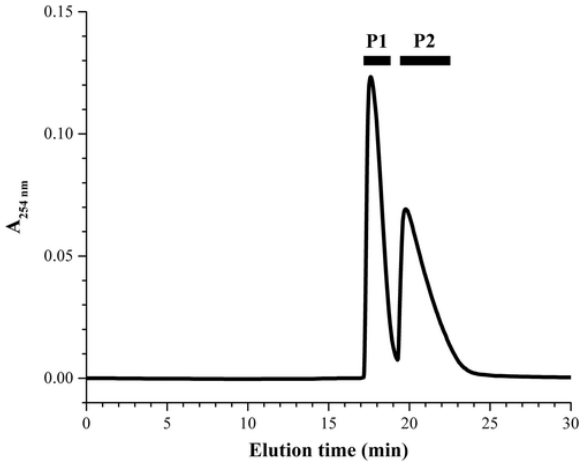

Figure 2 Preparative resolution of EPP enantiomers by chiral HPLC on a 10 × 250 mm Chiralcel OJ-H column. Sample: 0.25 ml of 40 mg/ml *rac*-EPP in MeOH. Flow rate: 1 ml/min (MeOH was used as an eluent). The collected fractions corresponding to the first peak (P1) and the second peak (P2) are shown with horizontal bars. See the MATERIALS AND METHODS for the separation conditions

Chromatographic resolution (R_s) can be calculated using Eq. 115:

$$R_s = \frac{t_R^{P2} - t_R^{P1}}{w_{1/2}^{P1} + w_{1/2}^{P2}}$$

(1)

where t_R are retention times and $w_{1/2}$ are widths at half of the height of the peaks corresponding to the enantiomers.

The R_s value calculated for our preparative separations using Eq. **1** is 0.75. However, visual inspection of the chromatogram (Figure **2**) indicates a nearly baseline resolution that would correspond to $R_s > 1$. Thus, the 0.75 value is likely to be an underestimation resulting from the asymmetric shape of the peaks.

The chromatographic resolution can also be calculated using the "10% valley" method (Eq. 2)[15]:

$$R_s = 0.1\left(\frac{\bar{h}}{h_V}\right)$$

(2)

where $\bar{h}$ is the mean height of the two peaks and h_V is the height of the valley between the peaks. Using this equation, the resolution of 1.28 was calculated for the chromatogram in Figure 2.

Repeated runs allowed us to obtain about 0.2 g of each enantiomer in pure form (ee 95.2–95.5% for fraction P1 and 99.0–99.3% for fraction P2, as determined by analytical chiral HPLC).

Far-UV CD spectroscopy (Figure **3**) was used to determine the signs of optical rotation of the resolved enantiomers. The P1 fraction shows a strong positive Cotton effect at around 214 nm and a much weaker positive Cotton effect at around 232 nm. The CD spectrum of the P2 fraction is essentially the same, except that the ellipticities are negative. Thus, when resolving *rac*-EPP on the Chiralcel OJ stationary phase in the polar organic mode, the first peak (EPP P1) corresponds to the (+)-enantiomer, and the second peak (EPP P2) corresponds to the (−)-enantiomer. It is instructive to note that the same elution order was observed in the reversed-phase mode (not shown).

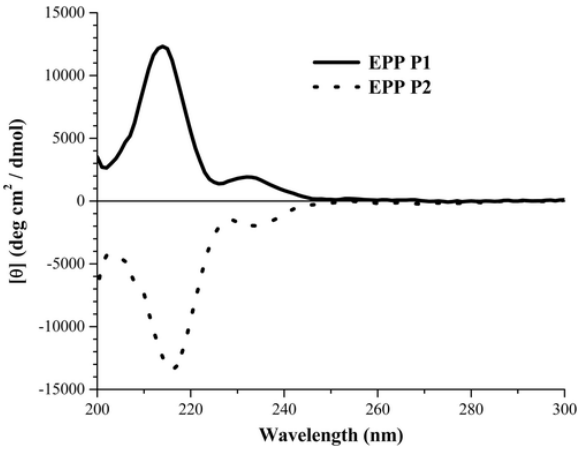

Figure 3 Far-UV CD spectra of EPP enantiomers resolved by chiral HPLC. Samples: 1-mM solutions of the first peak material (EPP P1) and the second peak material (EPP P2) in AcCN/H_2O (1:1). See the MATERIALS AND METHODS for the recording conditions

3.2 Determination of absolute configuration of EPP enantiomers

The structures of racemic and enantiopure forms of EPP were solved using single-crystal X-ray diffraction (Table **1**).

Table 1. Crystallographic data and structure refinement

Parameter	***rac*-EPP**	**(+)-(*R*)-EPP**	**(−)-(*S*)-EPP**
T, K	100.15	100.00	100.00
Radiation (*λ*), Å	0.71073	1.54184	1.54184
Crystal size, mm	1 × 0.492 × 0.172	0.38 × 0.32 × 0.25	0.25 × 0.22 × 0.18
Crystal system	monoclinic	orthorhombic	orthorhombic
Space group	$P2_1/c$	$P2_12_12_1$	$P2_12_12_1$
a, Å	11.6561(18)	8.51424(8)	8.51290(8)
b, Å	8.4419(13)	10.08673(9)	10.08769(11)
c, Å	10.7185(17)	11.69226(10)	11.68985(11)
α, deg.	90.00	90.00	90.00
β, deg.	105.151(2)	90.00	90.00
γ, deg.	90.00	90.00	90.00
V, Å^3	1018.0(3)	1004.142(15)	1003.871(17)
Z	4	4	4
ρ_{calc}, g/cm^3	1.235	1.252	1.252
μ, mm^{-1}	0.078	0.624	0.624
F(000)	408.0	408.0	408.0
2Θ range for data collection, deg.	3.62 to 61.1	11.58 to 148.16	11.58 to 148.18
Index ranges	−16 ≤ h ≤ 16	−10 ≤ h ≤ 10	−10 ≤ h ≤ 10
	−12 ≤ k ≤ 12	−12 ≤ k ≤ 12	−12 ≤ k ≤ 12
	−14 ≤ l ≤ 15	−14 ≤ l ≤ 14	−14 ≤ l ≤ 14
Reflections collected	10411	16156	14331
Independent reflections	3080	2035	2033
R_{int}	0.0205	0.0205	0.0206
R_{sigma}	0.0176	0.0101	0.0107

Data/restrains/parameters	3080 / 0 / 127	2035 / 0 / 129	2033 / 0 / 129
Goodness-of-fit on F^2	1.030	1.093	1.072
Final R indices, $I \geq 2\sigma(I)$	R_1 = 0.0385, wR_2 = 0.1071	R_1 = 0.0256, wR_2 = 0.0646	R_1 = 0.0253, wR_2 = 0.0634
Final R indices, all data	R_1 = 0.0413, wR_2 = 0.1098	R_1 = 0.0259, wR_2 = 0.0649	R_1 = 0.0257, wR_2 = 0.0637
Largest diff. peak / hole, e·Å^{-3}	0.43 / -0.20	0.23 / -0.13	0.22 / -0.13
Flack x parameter	not appl.	0.1(2)	0.0(2)
Hooft y parameter	not appl.	0.08(4)	0.01(5)
No. of Bijvoet pairs	not appl.	840 (99.6%)	838 (99.4%)

Absolute configuration of enantiomers can be inferred from anomalous dispersion (resonant scattering) of X-rays registered as the intensity difference between Bijvoet or Friedel pairs. For compounds that (like EPP) contain only light atoms (C, H, O, or N), such determinations tend to be challenging due to the inherently low intensity of anomalous dispersion for such atoms.[10, 16, 17] In order to increase the intensity of anomalous dispersion, we used CuKα radiation for X-ray diffraction measurements with the resolved enantiomers.

For a compound with a single chiral center (such as EPP), determining absolute configuration of one enantiomer is in principle sufficient to deduce the absolute configuration of the second enantiomer (antipode). However, in order to have a more reliable assignment, we independently determined the absolute configuration for each enantiomer.

Numerical expression of the differences between Friedel pairs for the purposes of an absolute structure assignment is most frequently accomplished using the Flack x parameter[9] (fitted during the refinement process). Recently, another—arguably more robust[18]—measure of anomalous dispersion, the Hooft y parameter[10] (calculated after refinement), was introduced. We calculated both of these parameters (Table **1**).

Flack and Bernardinelli[19] note that in order to reliably determine absolute configuration of an enantiopure compound, an uncertainty of the Flack x parameter, u, should be less than 0.1, and that, at $u > 0.3$, the R versus S distinguishing power is too weak for a reliable determination. Thus, the uncertainty in our Flack x parameter values (±0.2) is higher than that needed for a fully reliable determination of absolute configuration. This imprecision is very typical when the Flack parameter is calculated for light-atom structures, with the $u < 0.1$ situation being virtually unachievable (see, for example, Parsons et al.[17]).

As expected, about four times smaller uncertainty was obtained for the values of the Hooft parameter compared to the Flack parameter (Table **1**) allowing for a reliable determination of absolute configuration. Importantly, the values of the Flack and Hooft parameters for each enantiomer are in full agreement.

Thus, the values of the Hooft and Flack parameters indicate that EPP P1 is the (*R*)-enantiomer, and EPP P2 is the (*S*)-enantiomer. Taking into account the optical rotation signs observed in CD spectra (see above), EPP P1 can be assigned as (+)-(*R*)-EPP, and EPP P2 can be assigned as (−)-(*S*)-EPP.

3.3 Molecular and crystal structures of enantiopure and racemic forms of EPP

Naturally, the molecular structures of (+)-(*R*)-EPP and (−)-(*S*)-EPP are the mirror images of each other. Furthermore, the conformation of the EPP molecule in the racemic crystal is essentially the same as in enantiopure crystals (Figure **4**). The lactam heterocycle has a flattened envelope conformation. The deviation of the C3 atom from the mean plane of the remaining four atoms of the lactam ring is 0.45 Å for the enantiopure forms and 0.48 Å for the racemic form.

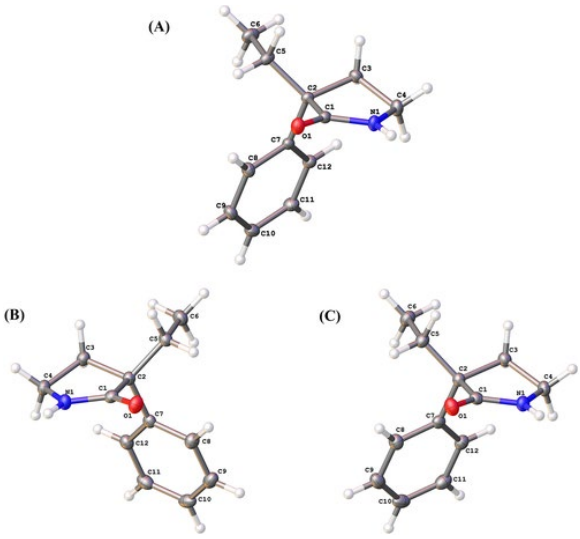

Figure 4 ORTEP diagrams of molecular structures of *rac*-EPP **A**, (+)-(*R*)-EPP **B**, and (−)-(*S*)-EPP (**C**)

The only conformational difference worth mentioning is the small (about 10 degrees) tilt of the phenyl group around the C2–C7 bond in the enantiopure forms relative to the racemate (Table **2**). This tilt is most probably caused by packing effects in crystals.

Table 2. Torsion angles (deg.) related to the orientation of the phenyl group in the crystal structures of EPP

Compound	C1-C2-C7-C8	C1-C2-C7-C12	C3-C2-C7-C8	C3-C2-C7-C12	C5-C2-C7-C8	C5-C2-C7-C12
rac-EPP	61.34(9)	−116.81(8)	171.43(7)	−6.72(10)	−58.72(9)	123.14(8)
(+)-(*R*)-EPP	−71.66(11)	−107.06(11)	177.25(9)	−4.04(14)	49.75(13)	−131.54(10)
(−)-(*S*)-EPP	71.68(12)	−107.09(11)	−177.24(9)	3.99(14)	−49.74(13)	131.49((10)

At the same time, dramatic differences were observed in supramolecular synthons and crystal structures of enantiopure and racemic forms of EPP (Figure **5**, Table **3**).

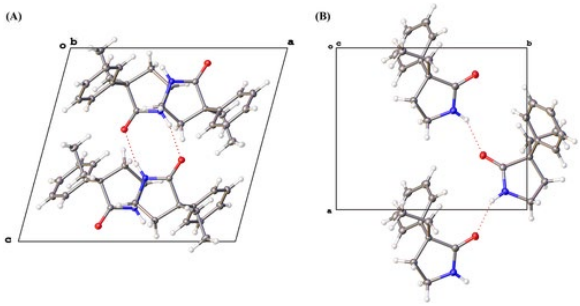

Figure 5 Supramolecular synthons in crystals of *rac*-EPP **A** and (+)-(*R*)-EPP **B**. NB: The structure of (−)-(*S*)-EPP is a mirror image of that of (+)-(*R*)-EPP, and, therefore, the former was omitted for clarity

Table 3. Intermolecular hydrogen bonds (Å and deg.) in the crystal structures of EPP

Compound	D - H…A	d(D - H)	d(H…A)	d(D…A)	∠(D - H…A)
rac-EPP	N1 - H1…O1[a]	0.88	2.01	2.8714(10)	164.4
(+)-(*R*)-EPP	N1 - H1…O1[b]	0.88	2.07	2.8422(12)	146.0
(−)-(*S*)-EPP	N1 - H1…O1[b]	0.88	2.07	2.8422(12)	145.9
3,3-diethylpyrrolidin-2-one	N1 - H1…O1[c]	0.86	2.07	2.902(3)	161.6

D, proton donor; A, proton acceptor.

H-bond parameters of an achiral lactam, 3,3-diethylpyrrolidin-2-one,[21] are given for comparison.

Symmetry transformations used to generate equivalent atoms:
[a] 1-*x*, 1-*y*, 1-*z*;
[b] 1/2 + *x*, 3/2-*y*, 1-*z*;
[c] 1-*x*, 2-*y*, −*z*.

Rac-EPP forms centrosymmetric dimers where the molecules are connected by N-H···O hydrogen bonds, thus forming eight-membered rings (Figure **4**, Table **3**). These dimers are similar to those formed by achiral 3,3-diethylpyrrolidin-2-one,[20, 21] by unsubstituted pyrrolidin-2-one at 173 K,[22] and by unsubstituted hexahydro-2*H*-azepin-2-one.[23] This is quite different from the one-dimensional zigzag chains with *syn* orientation of the phenyl rings relative to the lactam ring plane observed by Michon et al.[24] for racemic 3-allyl-3-phenylpiperidin-2-one.

(+)-(*R*)- and (−)-(*S*)-EPP, on the other hand, form one-dimensional zigzag chains similar to those we previously observed in the orthorhombic polymorphs of enantiopure forms of 3-methyl-3-phenylpyrrolidine-2,5-dione.[11]

The hydrogen bond parameters (Table **3**) in *rac*-EPP are very similar to those we previously observed in achiral 3,3-diethylpyrrolidin-2-one.[21] In enantiopure forms of EPP, the H-bond angle is substantially (by about 18 degrees) smaller than in the racemic form, resulting in a shorter donor-acceptor distance.

3.4 IR spectra of enantiopure and racemic forms of EPP

Solid-state IR spectra of *rac*-EPP and (+)-(*R*)-EPP are shown in Figure **6**; since the IR spectrum of (−)-(*S*)-EPP is identical to that of (+)-(*R*)-EPP, the former was omitted for clarity. Only the two most important spectral regions (corresponding to N-H and C=O stretching vibrations) are presented.

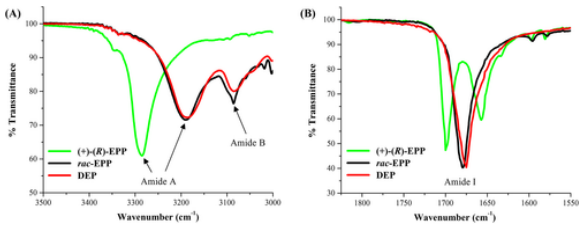

Figure 6 ATR IR spectra of EPP in the crystalline state. The N-H stretch region is shown in **A**, and the C=O stretch region is shown in **B**. See Table 4 for peak frequencies and assignments. For comparison, ATR IR spectrum of an achiral lactam, 3,3-diethylpyrrolidin-2-one (DEP),[21] is also shown. NB: The IR spectrum of (−)-(*S*)-EPP is identical to that of (+)-(*R*)-EPP, and, therefore, the former was omitted for clarity

The solid-state IR spectrum of *rac*-EPP has three main bands (Figure **6**, Table **4**): the main N-H stretch band at 3190 cm^{-1}, the additional 3086 cm^{-1} band (likely originating from Fermi resonance), and the C=O stretch band at 1679 cm^{-1}. This spectrum is very similar to that of 3,3-diethylpyrrolidin-2-one (DEP)[20] (cf. the black and red traces in Figure **6**) and also to the IR spectrum of neat (liquid) pyrrolidin-2-one,[25] suggesting that vibrational modes of the phenyl group do not make a major contribution to the observed IR spectrum of EPP. Very similar N-H (3209–3220 cm^{-1}) and C=O (1688–1700 cm^{-1}) frequencies were also observed in the solid state for racemic 3-phenylpyrrolidin-2-one in KBr pellets[26] and racemic 3-benzyl-3-ethylpyrrolidin-2-one on an NaCl plate.[27]

Table 4. Vibrational modes of EPP in the crystalline state

Vibrational mode	**IR frequency, cm^{-1}**		
	(+)-(*R*)- or (−)-(*S*)-EPP	***rac*-EPP**	**3,3-diethylpyrrolidin-2-one**
ν(N-H)	3286	3190	3185
ν(N-H)*	—	3086	3085
ν(C=O)	1657, 1700	1679	1675

IR frequencies of an achiral lactam, 3,3-diethylpyrrolidin-2-one,[21] are given for comparison.

* Fermi resonance between the ν(N-H) band and the ν(C=O) + δ(N-H) combination band.

The spectra of (+)-(*R*)-EPP and (−)-(*S*)-EPP are markedly different from the *rac*-EPP spectrum (Figure **6**, Table **4**); the main N-H stretch frequency increases by 96 cm^{-1}, the Fermi resonance band disappears, and the C=O stretch band splits into two.

One (superficially the most straightforward) explanation of the three different frequencies observed for the C=O stretch in EPP is to assign the 1700 cm^{-1} band to strongly H-bonded C=O groups (such as those in zigzag chains), the 1679 cm^{-1} band—to moderately H-bonded C=O groups (such as those in cyclic dimers), and the 1657 cm^{-1} band—to free C=O groups. However, if free C=O groups exist in enantiopure EPP crystals, then free N-H groups must be present at equimolar concentration. This implication is not compatible with the IR spectrum in the Amide A and Amide B region—as found by Hallam and Jones,[25, 28] free N-H groups would manifest themselves as a band at around 3455 cm^{-1}, but no such band is observed in any of the EPP samples (Figure **6**A).

In our opinion, a more likely explanation for the band splitting in the C=O stretch region of the enantiopure forms of EPP is the changes in hydrogen bond geometry and/or dipole–dipole coupling. Notably, an IR spectrum very similar to those of EPP enantiomers was observed for large-ring (capryllactam and larger) flexible lactams in which the amide group exists in *trans* configuration.[25] Of course, the amide group in EPP is in *cis* configuration (Figure **4**). Thus, we propose that the bands at 3285 cm^{-1} (N-H stretch) and 1700 and 1657 cm^{-1} (C=O stretch) are not due to *trans* configuration per se. Further spectroscopic and X-ray diffraction studies will be required to precisely define structural features responsible for the abovementioned vibrational modes.

3.5 Enantiopure forms of EPP have higher thermal stability than the racemic form

The melting point value for the EPP racemate (Table **5**) is the same as the one (88–90 °C) previously reported by Marshall.[5] It is also the same as the melting point of racemic 3-benzyl-3-ethylpyrrolidin-2-one (89–90 °C).[27]

Table 5. Bulk physicochemical properties of EPP in the crystalline state

Compound	Number of intermolecular H-bonds[a]	Density (g/cm^3)[a]	Melting point (°C)[b]
rac-EPP	2	1.235	89.8 ± 0.8
(+)-(*R*)-EPP	2	1.252	114.8 ± 0.3
(−)-(*S*)-EPP	2	1.252	115.0 ± 0.2

[a] From single-crystal X-ray diffraction data.
[b] Clear point, four to five independent measurements (M ± SD).

The melting points of the EPP enantiomers are about 25 °C higher than the melting point of *rac*-EPP (Table **5**) implying lower aqueous solubility. Notably, the corresponding increase in crystal density is small (0.02 g/cm^3). For comparison, crystals of enantiopure forms of 3-methyl-3-phenylpyrrolidine-2,5-dione have about 33 °C higher melting points and 0.09 g/cm^3 higher densities compared to the racemates crystals.[12] However, in the case of 4-phenyl-1,3-oxazolidine-2-thione,[29] the 46 °C higher melting point of its racemic form corresponds to a crystal density increase of only 0.05 g/cm^3.

The intramolecular H-bond length (D...A) in crystals formed by EPP enantiomers is about 0.03 Å shorter than in *rac*-EPP crystals (Table **3**). Thus, multiple factors (H-bond strength and directionality, cooperativity of H-bond formation and breakage, van der Waals interactions) likely contribute to the higher stability of the enantiopure crystals.

3.6 Possible pharmaceutical implications

Stereochemistry can influence pharmacological and pharmaceutical phenomena through three broad pathways:

i. Stereoselective binding of drugs to their targets (see Pfeiffer and Jenney[1] for some examples). We have recently discovered that α-substituted lactams, succinimides, and acetamides inhibit the function of neuronal nicotinic acetylcholine receptors.[30] It remains to be determined whether the inhibition of these receptors by α-substituted lactams is stereoselective (our preliminary data indicate that the inhibition by α-substituted succinimides and acetamides is not stereoselective).

ii. Stereoselective metabolism. We are not aware of any studies on the metabolism of α-substituted lactams (either racemic or enantiopure), so this is a completely unexplored area.

iii. Differences in solubility (and, therefore, in bioavailability) between racemic and enantiopure forms. There are many examples of such differences.[2]

Pharmacokinetic profiling of racemic and enantiopure forms of a drug (e.g., EPP) in rats upon oral administration versus i.v. administration can be used to determine bioavailability. The pharmaceutically relevant solubility differences between racemic and enantiopure forms can also be quantified in vitro by comparing the dissolution kinetics. So far, no such studies have been reported for any α-substituted lactam—possibly due to the fact that fairly large, gram quantities of pure enantiomers would be required. We hope that the results we report in this article (e.g., the scalable separation conditions for chiral HPLC and the knowledge of the relationship between the easily measurable sign of optical rotation and the absolute configuration) will pave the road to such studies. Given the structural differences discussed above, we expect that the racemic form of EPP will have higher bioavailability than its enantiopure forms.

4 CONCLUSION

The key outcomes of our study are as follows:

- Enantiomers of an experimental AED 3-ethyl-3-phenylpyrrolidin-2-one (EPP) have been resolved on a preparative scale by chiral HPLC on the Chiralcel OJ stationary phase in the polar-organic mode.
- Using a combination of single-crystal X-ray diffraction and far-UV CD spectroscopy, we established that the peak eluting first corresponds to (+)-(*R*)-EPP and the peak eluting second corresponds to (−)-(*S*)-EPP. The use of the Hooft *y* parameter allowed us to reliably assign absolute configurations of these challenging light-atom molecules.
- Crystal structures of both enantiopure and racemic forms of EPP are based on H-bonded supramolecular synthons. However, stereospecific differences in the nature of these synthons were observed: *rac*-EPP forms cyclic dimers, while (+)-(*R*)-EPP and (−)-(*S*)-EPP form one-dimensional infinite zigzag chains.
- The dramatic differences in the crystal structures of enantiopure and racemic forms of EPP are corroborated by the corresponding differences in IR spectra and melting points.
- These stereospecific structural differences in the solid state will translate into different solubilities and bioavailabilities and should thus be kept in mind during the development of pharmaceutical formulations for EPP and related AEDs.

ACKNOWLEDGMENTS

We thank Dr. Vladimir V. Ermolenkov (University at Albany, SUNY, Albany, NY) for help with recording the CD spectra and Dr. Martha A. Hass (Albany College of Pharmacy and Health Sciences, Albany, NY) for the use of her FT-IR spectrometer. Funding from the University of Houston – Clear Lake Faculty Research Support Fund (grant FRSF#1176, to A.V.K.), National Science Foundation (PREM program, DMR 1523611 grant, to T.V.T.), and the

Ministry of Education and Science of the Russian Federation (contract 02.a03.21.0008, to V.N.K. and Vladimir M. Filippov) is gratefully acknowledged.

REFERENCES

1 Pfeiffer CC, Jenney EH. Natural asymmetry, isomerism and pharmacological action. *J Sci Ind Res*. 1967; **26**: 29- 34.
2 Gu C-H, Grant DJW. Effects of crystal structure and physical properties on the release of chiral drugs. In: IK Reddy, R Mehvar, eds. *Chirality in Drug Design and Development*. New York: Marcel Dekker; 2004: 1- 33.
3 Ngugi AK, Bottomley C, Kleinschmidt I, Sander JW, Newton CR. Estimation of the burden of active and life-time epilepsy: A meta-analytic approach. *Epilepsia*. 2010; **51**: 883- 890.
4 Krivoshein AV. Antiepileptic drugs based on the α-substituted amide group pharmacophore: From chemical crystallography to molecular pharmaceutics. *Curr Pharm Des*. 2016; **22**: 5029- 5040.
5 Marshall FJ. Some 3,3-substituted-2-pyrrolidinones. *J Org Chem*. 1958; **23**: 503- 505.
6 Gruber CM, Mosier JM, Gibson WR. Drugs and epilepsy—motor seizures. *Arch Int Pharmacodyn*. 1959; **121**: 443- 458.
7 Sheldrick GM. Crystal structure refinement with SHELX. *Acta Crystallogr*. 2015; **A71**: 3- 8.
8 Dolomanov OV, Bourhis LJ, Gildea RJ, Howard JAK, Puschmann H. OLEX2: A complete structure solution, refinement and analysis program. *J Appl Cryst*. 2009; **42**: 339- 341.
9 Flack HD. On enantiomorph-polarity estimation. *Acta Crystallogr*. 1983; **A39**: 876- 881.
10 Hooft RWW, Straver LH, Spek AL. Determination of absolute structure using Bayesian statistics on Bijvoet differences. *J Appl Cryst*. 2008; **41**: 96- 103.
11 Spek AL. Structure validation in chemical crystallography. *Acta Crystallogr*. 2009; **D65**: 148- 165.
12 Khrustalev VN, Sandhu B, Bentum S, Fonari A, Krivoshein AV, Timofeeva TV. Absolute configuration and polymorphism of 2-phenylbutyramide and α-methyl-α-phenylsuccinimide. *Cryst Growth Des*. 2014; **14**: 3360- 3369.
13 Miller L, Orihuela C, Fronek R, Murphy J. Preparative chromatographic resolution of enantiomers using polar organic solvents with polysaccharide chiral stationary phases. *J Chromatogr A*. 1999; **865**: 211- 226.
14 Matthijs N, Maftouh M, Heyden YV. Screening approach for chiral separation of pharmaceuticals. IV. Polar organic solvent chromatography. *J Chromatogr A*. 2006; **1111**: 48- 61.
15 Braithwaite A, Smith FJ. *Chromatographic Methods*. 5th ed. Dordrecht, Netherlands: Kluwer Academic Publishers; 1999: 37- 38.
16 Flack HD, Bernardinelli G. The use of X-ray crystallography to determine absolute configuration. *Chirality*. 2008; **20**: 681- 690.
17 Parsons S, Flack HD, Wagner T. Use of intensity quotients and differences in absolute structure refinement. *Acta Crystallogr*. 2013; **B69**: 249- 259.
18 Watkin DJ, Cooper RI. Why direct and post-refinement determinations of absolute structure may give different results. *Acta Crystallogr*. 2016; **B72**: 661- 683.
19 Flack HD, Bernardinelli G. Reporting and evaluating absolute-structure and absolute-configuration determinations. *J Appl Cryst*. 2000; **33**: 1143- 1148.
20 Cohen-Addad C. Diéthylacétamide. *Acta Cryst*. 1979; **B35**: 2471- 2472.
21 Krivoshein AV, Ordonez C, Khrustalev VN, Timofeeva TV. Distinct molecular structures and hydrogen bond patterns of α,α-diethyl-substituted cyclic imide, lactam, and acetamide derivatives in the crystalline phase. *J Mol Struct*. 2016; **1121**: 196- 202.
22 Goddard R, Heinemann O, Krüger C, Magdó I, Mark F, Schaffner K. A low-temperature phase of 2-pyrrolidone. *Acta Crystallogr*. 1998; **C54**: 501- 504.
23 Winkler FK, Dunitz JD. Medium-ring compounds. XIX. Caprolactam: Structure refinement. *Acta Crystallogr*. 1975; **B31**: 268- 269.
24 Michon C, Béthegnies A, Capet F, et al. Catalytic asymmetric allylic alkylation of 3-arylated piperidin-2-ones. *Eur J Org Chem*. 2013; 4979- 4985.

25 Hallam HE, Jones CM. Structures of cyclic amides. Part 2. Associated species. *J Mol Struct*. 1967–68; **1**: 425- 435.
26 Bertozzi S, Salvadori P. Synthesis of 3-phenyl- and 5-phenyl-2-pyrrolidinone via rhodium catalysed carbonylation of allylamines. *Synth Commun*. 1996; **26**: 2959- 2965.
27 Reddy PA, Hsiang BCH, Latifi TN, et al. 3,3-Dialkyl- and 3-alkyl-3-benzyl-substituted 2-pyrrolidinones: A new class of anticonvulsant agents. *J Med Chem*. 1996; **39**: 1898- 1906.
28 Hallam HE, Jones CM. Structures of cyclic amides. Part 1. Monomeric species. *J Mol Struct*. 1967–68; **1**: 413- 423.
29 Kitoh S, Kunimoto K, Funaki N, Senda H, Kuwae A, Hanai K. Crystal structures and vibrational spectra of racemic and chiral 4-phenyl-1,3-oxazolidine-2-thione. *J Chem Crystallogr*. 2002; **32**: 547- 553.
30 Krivoshein AV. Anticonvulsants based on the α-substituted amide group pharmacophore bind to and inhibit function of neuronal nicotinic acetylcholine receptors. *ACS Chem Nerosci*. 2016; **7**: 316- 326.